

Figure S1. **Structure-function studies revealed the functions of LIM domains of paxillin in invadosome morphometry and dynamics.** (A) Morphometric analysis (surface, perimeter, and thickness) of the invadosome induced by either pax-Flag-WT or pax-ΔLIM-Flag mutant expressed in MEF-SrcY527F pax^{-/-} shHic-5 cells (50 invadosome rings were quantified per condition). a.u., arbitrary units. (B) Representative images extracted from the time series of MEF-SrcY527F pax^{-/-} shHic-5 cells expressing LifeAct-GFP revealed a highly dynamic invadosome turnover (multicolored arrowheads) in the presence of pax-Flag-WT, whereas the pax-ΔLIM-Flag mutant induced long-lasting poorly dynamic large rings (red arrowhead). (C) Representative images of a FRAP experiment (same imaging conditions and setup) on MEF-SrcY527F cells expressing GFP-actin in the presence of pax-Flag-WT and pax-ΔLIM-Flag. Red rectangles show the area where the photobleaching is induced. Quantification of GFP-actin characteristic time of recovery showed that pax-ΔLIM-Flag stabilized actin dynamics in invadosomes in comparison with pax-WT-Flag. ***, P < 0.001. Bars, 4 μm.

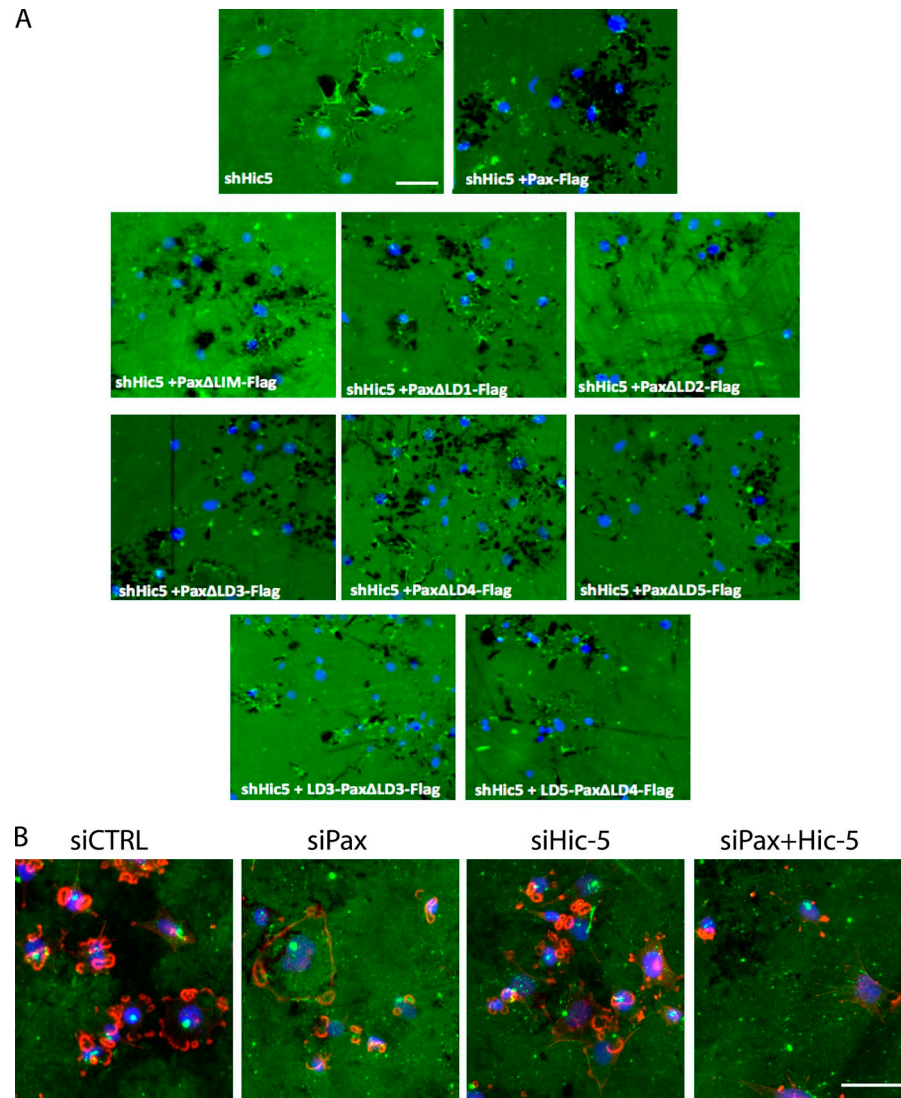


Figure S2. **Representative ECM degradation patterns.** (A) Representative micrographs of MEF-SrcY527F *pax*^{-/-} shHic-5 cells expressing different paxillin mutants and spread on Oregon-green gelatin layer for 10 h. Cells were fixed and stained for DAPI before imaging with a 10x objective to measure ECM degradation, normalized to the number of nuclei in large cell numbers. (B) Representative micrographs of MEF-SrcY527F cells treated with the indicated siRNA before being spread on Oregon-green gelatin layer for 10 h, fixed, and stained for DAPI and F-actin-TRITC. Bars: (A) 50 μ m; (B) 25 μ m.

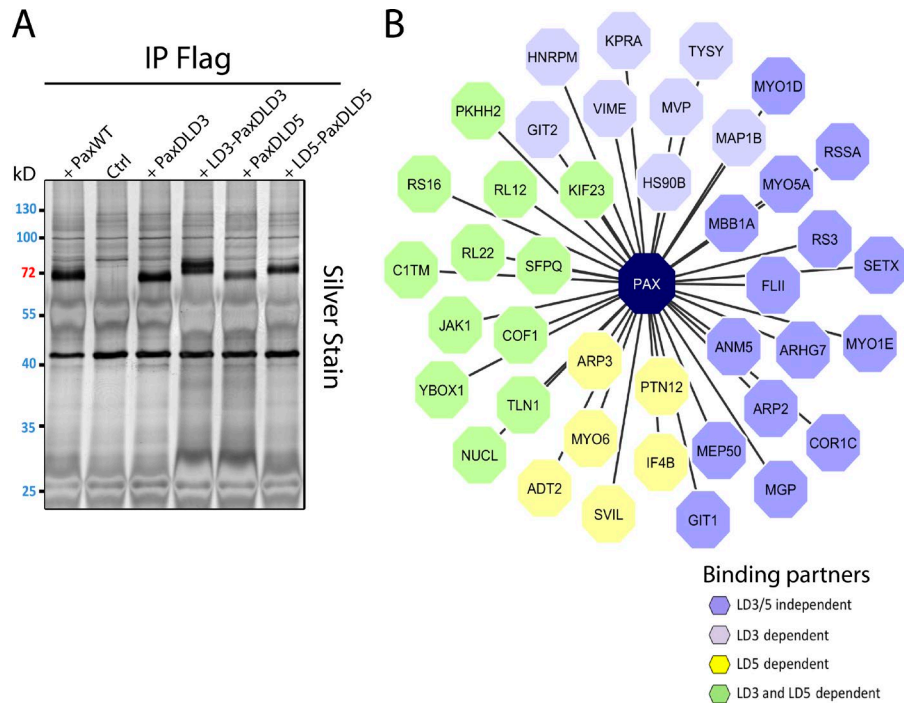


Figure S3. **Specific LD3 and LD5 interactors of paxillin.** (A) SDS-PAGE (10% gel) and silver staining analysis of paxillin binding partners copurified with pax-WT-Flag, pax-Flag mutants deleted for LD3 or LD5, and pax-Flag mutants pax-LD3_ΔLD3-Flag or pax-LD5_ΔLD5-Flag using an anti-flag M2 antibody. The control condition corresponds to cell lysates of paxillin-deficient cells (pax^{-/-} and Hic-5^{-/-} cells) with nonspecific IgG but the same isotype as anti-Flag M2. (B) Protein interaction diagram of all interactors of paxillin. Based on a comparative study of the interactors of pax-WT-Flag and pax-Flag mutants deleted for LD3 or LD5, it was possible to identify the interactors independent of LD3 and LD5, dependent on LD3, dependent on LD5, and dependent on LD3 and LD5.

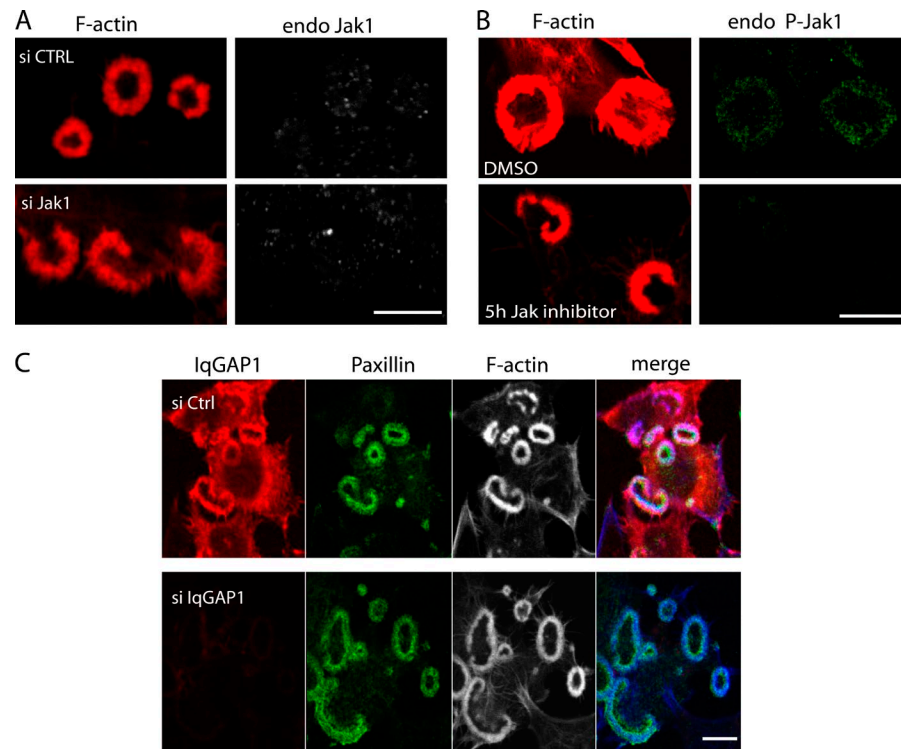


Figure S4. **Specific localization of endogenous JAK1 or IQGAP1 in invadosome.** (A) Confocal imaging of F-actin and endogenous JAK1 (total JAK1) in MEF-SrcY527F cells treated with CTRL or specific JAK1 siRNA. Cells were fixed and stained with the same procedure before performing quantitative confocal imaging performed with the same optical path and setup of the photomultiplier tube to compare fluorescence intensity. (B) The same protocol was applied on MEF-SrcY527F cells treated with DMSO or Jak inhibitor I for 5 h before fixation and staining with a specific antibody against phospho-JAK1. (C) Confocal imaging of endogenous IQGAP1 in MEF-SrcY527F cells treated with control or specific IQGAP1 siRNA. Silencing of IQGAP1 in MEF SrcY527F cells validates the specificity of endogenous IQGAP1 immunodetection (red staining), which was highly enriched in invadosome rings (visualized by paxillin staining in green). Bars: (A and B) 5 μ m; (C) 8 μ m.

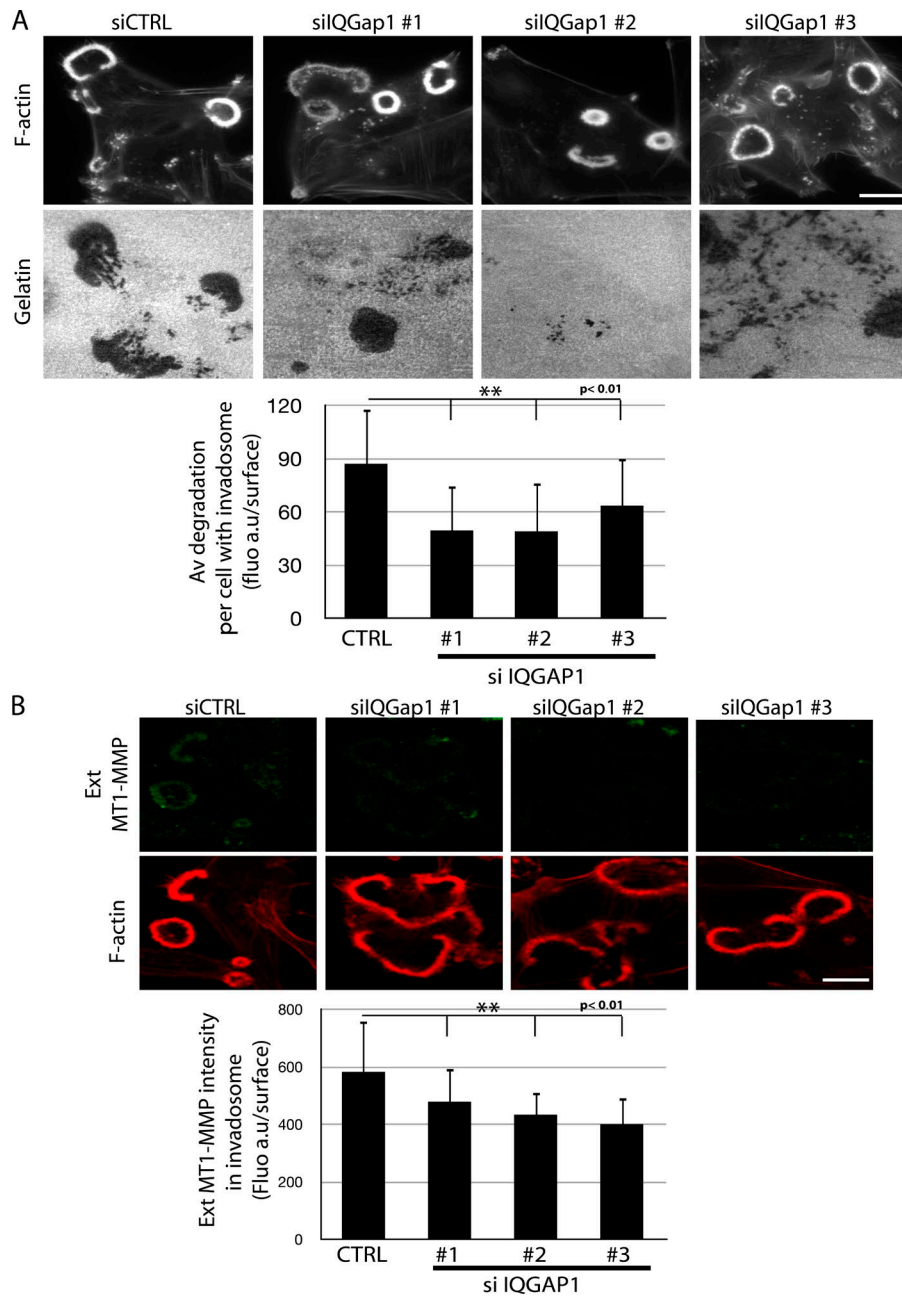


Figure S5. **IQGAP1 silencing decreases ECM degradation of MEF-SrcY527F cells and is associated with a decrease of MT1-MMP at the surface of invadosomes.** (A) F-actin staining of cells treated by different IQGAP siRNAs and spread on fluorescent gelatin layer for 12 h. IQGAP1 silencing induces large invadosomes that poorly digest ECM in comparison to control cells. To quantify this effect, the mean value (fluorescence in arbitrary units [fluorescence a.u.]/surface) of the digested ECM was quantified under cells forming invadosomes (representative of three different experiments, 50–75 cells per condition). (B) Based on the ability of MT1-MMP antibody to recognize the extracellular domain of this protease, its surface expression was detected in MEF-SrcY527F cells treated by different IQGAP siRNAs. Cells were fixed and stained without permeabilization and with the same procedure before performing quantitative confocal imaging. The same optical path and setup of the photomultiplier tube have been used to compare fluorescence intensity. Note the decrease of MT1-MMP accumulation after IQGAP1 depletion. **, $P < 0.01$. Bars: (A) 4 μ m; (B) 3 μ m.

Table S1. **Specific interactors of Hic-5-WT-Flag**

| Protein abbreviation | Negative control | Hic-5-WT-Flag | Protein name |
|----------------------|------------------|---------------|--|
| ANM5_MOUSE | 0.0 | 9.5 | Protein arginine N-methyltransferase 5 |
| ARP2_MOUSE | 0.5 | 4.0 | Actin-related protein 2 |
| DDB1_MOUSE | 0.5 | 2.5 | DNA damage-binding protein 1 |
| DJB11_MOUSE | 0.0 | 3.5 | DnaJ homolog subfamily B member 11 |
| EF1D_MOUSE | 0.5 | 2.5 | Elongation factor 1-δ |
| FLIL_MOUSE | 0.0 | 6.5 | Protein flightless-1 homolog |
| GIT1_MOUSE | 0.0 | 2.5 | ARF GTPase-activating protein GIT1 |
| GLYR1_MOUSE | 1.0 | 5.0 | Putative oxidoreductase GLYR1 |
| IQGAP1_MOUSE | 0.5 | 2.5 | Ras GTPase-activating-like protein IQGAP1 |
| KPRA_MOUSE | 0.0 | 5.5 | Phosphoribosyl pyrophosphate synthase-associated protein 1 |
| LRRF1_MOUSE | 0.0 | 2.5 | Leucine-rich repeat flightless-interacting protein 1 |
| MBB1A_MOUSE | 1.0 | 7.0 | Myb-binding protein 1A |
| MEP50_MOUSE | 0.0 | 4.0 | Methylosome protein 50 |
| MGP_MOUSE | 0.0 | 2.5 | Matrix Gla protein |
| NPM_MOUSE | 0.5 | 3.5 | Nucleophosmin |
| PRPS1_MOUSE | 0.0 | 2.5 | Ribose-phosphate pyrophosphokinase 1 |
| PTN12_MOUSE | 0.0 | 9.0 | Tyrosine-protein phosphatase nonreceptor type 12 |
| QOVEI6_MOUSE | 0.0 | 6.0 | Advillin |
| RBM39_MOUSE | 0.0 | 2.0 | RNA-binding protein 39 |
| RSSA_MOUSE | 0.0 | 3.0 | 40S ribosomal protein SA |
| SERPH_MOUSE | 0.0 | 3.0 | Serpin H |
| TOP2A_MOUSE | 0.0 | 6.0 | DNA topoisomerase 2-α |
| TR150_MOUSE | 0.5 | 3.0 | Thyroid hormone receptor-associated protein 3 |
| TGFI1_MOUSE | 0.0 | 36.0 | Hic-5 |

Table S2. Specific interactors of pax-WT-Flag

| Protein abbreviation | Negative control | Pax-WT-Flag | Protein name |
|----------------------|------------------|-------------|--|
| ADT2_MOUSE | 0.3 | 1.7 | ADP/ATP translocase 2 |
| ANM5_MOUSE | 0.0 | 15.0 | Protein arginine N-methyltransferase 5 |
| ARHG7_MOUSE | 0.0 | 5.7 | Rho guanine nucleotide exchange factor 7 (Beta-Pix) |
| ARP2_MOUSE | 0.3 | 2.0 | Actin-related protein 2 |
| ARP3_MOUSE | 0.3 | 2.3 | Actin-related protein 3 |
| B1ASP2_MOUSE | 0.3 | 3.0 | Tyrosine-protein kinase-JAK1 |
| C1TM_MOUSE | 0.3 | 2.3 | Monofunctional C1-tetrahydrofolate synthase. |
| COF1_MOUSE | 0.3 | 2.7 | Cofilin-1 (Cofilin, nonmuscle isoform) |
| COR1C_MOUSE | 0.3 | 3.3 | Coronin-1C (Coronin-3) |
| E9Q175_MOUSE | 0.0 | 3.0 | Unconventional myosin-VI |
| E9Q5G3_MOUSE | 0.0 | 2.7 | Protein Kif23 |
| FLII_MOUSE | 0.0 | 7.3 | Protein flightless-1 homolog |
| GIT1_MOUSE | 0.0 | 7.0 | ARF GTPase-activating protein GIT1 |
| GIT2_MOUSE | 0.0 | 2.3 | ARF GTPase-activating protein GIT2 |
| HNRPM_MOUSE | 1.7 | 9.0 | Heterogeneous nuclear ribonucleoprotein |
| HS90B_MOUSE | 0.0 | 3.0 | Heat shock protein HSP 90-β |
| IF4B_MOUSE | 0.7 | 4.3 | Eukaryotic translation initiation factor 4B |
| KPRA_MOUSE | 0.0 | 3.3 | Phosphoribosyl pyrophosphate synthase-associated protein 1 |
| MAP1B_MOUSE | 0.0 | 3.3 | Microtubule-associated protein 1B |
| MBB1A_MOUSE | 1.3 | 8.7 | Myb-binding protein |
| MEP50_MOUSE | 0.0 | 8.0 | Methylosome protein 50 |
| MGP_MOUSE | 0.0 | 3.0 | Matrix Gla protein |
| MVP_MOUSE | 0.7 | 4.3 | Major vault protein |
| MYO1D_MOUSE | 1.3 | 10.3 | Unconventional myosin-IId |
| MYO1E_MOUSE | 0.3 | 7.0 | Unconventional myosin-Ie |
| MYO5A_MOUSE | 0.0 | 6.0 | Unconventional myosin-Va |
| NUCL_MOUSE | 1.0 | 5.0 | Nucleolin |
| PKHH2_MOUSE | 0.0 | 3.0 | Pleckstrin homology domain-containing family |
| PTN12_MOUSE | 0.0 | 2.0 | Tyrosine-protein phosphatase non-receptor type 12 |
| RL12_MOUSE | 0.3 | 1.7 | 60S ribosomal protein L12 |
| RL22_MOUSE | 0.3 | 2.3 | 60S ribosomal protein L22 |
| RS16_MOUSE | 0.3 | 1.7 | 40S ribosomal protein S16 |
| RS3_MOUSE | 0.3 | 2.0 | 40S ribosomal protein S3 |
| RSSA_MOUSE | 0.0 | 2.0 | 40S ribosomal protein SA |
| SETX_MOUSE | 0.0 | 5.3 | Probable helicase senataxin |
| SFPQ_MOUSE | 0.3 | 2.0 | Splicing factor, proline- and glutamine-rich |
| SVIL_MOUSE | 0.0 | 2.3 | Supervillin (Archvillin; p205/p250) |
| TLN1_MOUSE | 0.0 | 2.0 | Talin-1 |
| TYSY_MOUSE | 0.0 | 2.0 | Thymidylate synthase |
| VIME_MOUSE | 1.0 | 10.3 | Vimentin |
| YBOX1_MOUSE | 0.0 | 2.0 | Nuclease-sensitive element-binding protein |
| PXN_MOUSE | 0.7 | 44.0 | Paxillin |

Table S3. Specific interactors of pax-WT-Flag, pax-ΔLD3-Flag, pax-ΔLD5-Flag, pax-LD3_ΔLD3-Flag, and pax-LD5_ΔLD5-Flag

| Protein abbreviation | Negative control | Pax-WT-Flag | Pax-ΔLD3-Flag | Pax-LD3_ΔLD3-Flag | Pax-ΔLD5-Flag | Pax-LD5_ΔLD5-Flag | Protein name |
|----------------------|------------------|-------------|---------------|-------------------|---------------|-------------------|--|
| ADT2_MOUSE | 0.3 | 1.7 | 3.0 | 0.0 | 0.0 | 0.0 | ADP/ATP translocase 2 |
| ANM5_MOUSE | 0.0 | 15 | 15 | 0.0 | 14.5 | 0.0 | Protein arginine N-methyltransferase 5 |
| ARHG7_MOUSE | 0.0 | 5.7 | 8.0 | 7.0 | 6.0 | 9.0 | Rho guanine nucleotide exchange factor 7 (Beta-Pix) |
| ARP2_MOUSE | 0.3 | 2.0 | 2.5 | 0.0 | 2.0 | 0.0 | Actin-related protein 2 |
| ARP3_MOUSE | 0.3 | 2.3 | 2.5 | 0.0 | 0.0 | 0.0 | Actin-related protein 3 |
| AVIL_MOUSE | 0.0 | 0.0 | 2.5 | 0.0 | 6.0 | 0.0 | Advillin |
| B1ASP2_MOUSE | 0.3 | 3.0 | 0.0 | 0.0 | 0.0 | 0.0 | Tyrosine-protein kinase-JAK1 |
| C1TM_MOUSE | 0.3 | 2.3 | 0.0 | 0.0 | 0.0 | 0.0 | Monofunctional C1-tetrahydrofolate synthase |
| COF1_MOUSE | 0.3 | 2.7 | 0.0 | 0.0 | 0.0 | 0.0 | Cofilin-1 (Cofilin, non-muscle isoform) |
| COR1C_MOUSE | 0.3 | 3.3 | 5.0 | 0.0 | 5.5 | 0.0 | Coronin-1C (Coronin-3) |
| DHX9_MOUSE | 0.0 | 0.0 | 0.0 | 0.0 | 2.5 | 0.0 | ATP-dependent RNA helicase A |
| DJB11_MOUSE | 0.0 | 0.0 | 0.0 | 3.0 | 0.0 | 0.0 | DnaJ homolog subfamily B member 11 |
| DNJA2_MOUSE | 0.0 | 0.0 | 0.0 | 0.0 | 2.0 | 0.0 | DnaJ homolog subfamily A member 2 |
| DPYL3_MOUSE | 0.0 | 0.0 | 0.0 | 0.0 | 0.0 | 3.0 | Dihydropyrimidinase-related protein 3 (DRP-3) |
| E9Q175_MOUSE | 0.0 | 3.0 | 0.0 | 0.0 | 0.0 | 0.0 | Unconventional myosin-VI |
| E9Q5G3_MOUSE | 0.0 | 2.7 | 0.0 | 0.0 | 0.0 | 0.0 | Protein Kif23 |
| ENOA_MOUSE | 1.0 | 0.0 | 0.0 | 0.0 | 0.0 | 5.0 | Alpha-enolase (EC 4.2.1.11) |
| FLII_MOUSE | 0.0 | 7.3 | 4.5 | 5.0 | 5.0 | 0.0 | Protein flightless-1 homolog |
| GIT1_MOUSE | 0.0 | 7.0 | 7.0 | 4.0 | 3.0 | 5.0 | ARF GTPase-activating protein GIT1 |
| GIT2_MOUSE | 0.0 | 2.3 | 0.0 | 3.0 | 2.5 | 0.0 | ARF GTPase-activating protein GIT2 |
| H2AV_MOUSE | 0.0 | 0.0 | 2.5 | 0.0 | 0.0 | 0.0 | Histone H2A.V |
| H2AX_MOUSE | 0.0 | 0.0 | 2.5 | 0.0 | 0.0 | 0.0 | Histone H2A.x |
| H32_MOUSE | 0.0 | 0.0 | 2.0 | 0.0 | 0.0 | 2.0 | Histone H3.2 |
| H4_MOUSE | 0.0 | 0.0 | 8.5 | 0.0 | 9.5 | 0.0 | Histone H4 |
| HNRPM_MOUSE | 1.7 | 9.0 | 0.0 | 0.0 | 16 | 0.0 | Heterogeneous nuclear ribonucleo-protein |
| HS90B_MOUSE | 0.0 | 3.0 | 0.0 | 0.0 | 3.5 | 0.0 | Heat shock protein HSP 90-β |
| IF4B_MOUSE | 0.7 | 4.3 | 5.5 | 0.0 | 0.0 | 0.0 | Eukaryotic translation initiation factor 4B |
| KPRA_MOUSE | 0.0 | 3.3 | 0.0 | 0.0 | 2.5 | 6.0 | Phosphoribosyl pyrophosphate synthase-associated protein 1 |
| LDHA_MOUSE | 0.0 | 0.0 | 0.0 | 0.0 | 0.0 | 2.0 | L-lactate dehydrogenase A chain |
| LMNA_MOUSE | 0.0 | 0.0 | 0.0 | 0.0 | 3.5 | 0.0 | Prelamin-A/C |
| MAP1B_MOUSE | 0.0 | 3.3 | 0.0 | 0.0 | 2.5 | 0.0 | Microtubule-associated protein 1B |
| MBB1A_MOUSE | 1.3 | 8.7 | 6.0 | 0.0 | 6.5 | 0.0 | Myb-binding protein 1A |
| MED1_MOUSE | 0.0 | 0.0 | 0.0 | 4.0 | 0.0 | 0.0 | Mediator of RNA polymerase II transcription subunit 1 |
| MED12_MOUSE | 0.0 | 0.0 | 0.0 | 3.0 | 0.0 | 0.0 | Mediator of RNA polymerase II transcription subunit 12 |
| MED14_MOUSE | 0.0 | 0.0 | 0.0 | 2.0 | 0.0 | 0.0 | Mediator of RNA polymerase II transcription subunit 14 |
| MED15_MOUSE | 0.0 | 0.0 | 0.0 | 3.0 | 0.0 | 0.0 | Mediator of RNA polymerase II transcription subunit 15 |
| MED17_MOUSE | 0.0 | 0.0 | 0.0 | 3.0 | 0.0 | 0.0 | Mediator of RNA polymerase II transcription subunit 17 |
| MED23_MOUSE | 0.0 | 0.0 | 0.0 | 5.0 | 0.0 | 0.0 | Mediator of RNA polymerase II transcription subunit 23 |
| MED24_MOUSE | 0.0 | 0.0 | 0.0 | 6.0 | 0.0 | 0.0 | Mediator of RNA polymerase II transcription subunit 24 |
| MED31_MOUSE | 0.0 | 0.0 | 0.0 | 2.0 | 0.0 | 0.0 | Mediator of RNA polymerase II transcription subunit 31 |
| MEP50_MOUSE | 0.0 | 8.0 | 8.5 | 0.0 | 4.0 | 0.0 | Methylosome protein 50 |
| MGP_MOUSE | 0.0 | 3.0 | 3.0 | 0.0 | 3.0 | 0.0 | Matrix Gla protein |
| MVP_MOUSE | 0.7 | 4.3 | 0.0 | 0.0 | 5.0 | 0.0 | Major vault protein |
| MYL9_MOUSE | 0.0 | 0.0 | 0.0 | 0.0 | 0.0 | 5.0 | Myosin regulatory light polypeptide 9 |
| MYO1D_MOUSE | 1.3 | 10.3 | 12 | 0.0 | 15 | 0.0 | Unconventional myosin-IId |
| MYO1E_MOUSE | 0.3 | 7.0 | 9.0 | 0.0 | 7.0 | 0.0 | Unconventional myosin-Ie |
| MYO5A_MOUSE | 0.0 | 6.0 | 9.0 | 0.0 | 7.5 | 0.0 | Unconventional myosin-Va |

Table S3. Specific interactors of pax-WT-Flag, pax-ΔLD3-Flag, pax-ΔLD5-Flag, pax-LD3_ΔLD3-Flag, and pax-LD5_ΔLD5-Flag (Continued)

| Protein abbreviation | Negative control | Pax-WT-Flag | Pax-ΔLD3-Flag | Pax-LD3_ΔLD3-Flag | Pax-ΔLD5-Flag | Pax-LD5_ΔLD5-Flag | Protein name |
|----------------------|------------------|-------------|---------------|-------------------|---------------|-------------------|--|
| MYO6_MOUSE | 0.0 | 0.0 | 2.5 | 0.0 | 0.0 | 0.0 | Unconventional myosin-VI |
| NPM_MOUSE | 0.0 | 0.0 | 0.0 | 0.0 | 2.5 | 0.0 | Nucleophosmin |
| NUCL_MOUSE | 1.0 | 5.0 | 0.0 | 0.0 | 0.0 | 0.0 | Nucleolin |
| OAT_MOUSE | 0.0 | 0.0 | 0.0 | 0.0 | 0.0 | 2.0 | Ornithine aminotransferase, mitochondrial |
| PGK1_MOUSE | 0.0 | 0.0 | 0.0 | 0.0 | 0.0 | 2.0 | Phosphoglycerate kinase 1 (EC 2.7.2.3) |
| PKHH2_MOUSE | 0.0 | 3.0 | 0.0 | 0.0 | 0.0 | 2.0 | Pleckstrin homology domain-containing family H member 2 |
| PPIA_MOUSE | 0.0 | 0.0 | 0.0 | 0.0 | 0.0 | 2.0 | Peptidyl-prolyl cis-trans isomerase A |
| PTN12_MOUSE | 0.0 | 2.0 | 2.0 | 0.0 | 0.0 | 5.0 | Tyrosine-protein phosphatase non-receptor type 12 (EC 3.1.3.48; MPTP-PEST) |
| RBM39_MOUSE | 0.0 | 0.0 | 0.0 | 0.0 | 0.0 | 2.0 | RNA-binding protein 39 |
| RL5_MOUSE | 0.0 | 0.0 | 0.0 | 0.0 | 2.0 | 0.0 | 60S ribosomal protein L5 |
| RL7_MOUSE | 0.0 | 0.0 | 0.0 | 0.0 | 3.5 | 0.0 | 60S ribosomal protein L7 |
| RL7A_MOUSE | 0.0 | 0.0 | 0.0 | 0.0 | 2.5 | 0.0 | 60S ribosomal protein L7a |
| RL12_MOUSE | 0.3 | 1.7 | 0.0 | 0.0 | 0.0 | 0.0 | 60S ribosomal protein L12 |
| RL15_MOUSE | 0.0 | 0.0 | 0.0 | 0.0 | 0.0 | 2.0 | 60S ribosomal protein L15 |
| RL22_MOUSE | 0.3 | 2.3 | 0.0 | 0.0 | 0.0 | 0.0 | 60S ribosomal protein L22 |
| RLA1_MOUSE | 0.0 | 0.0 | 0.0 | 2.0 | 0.0 | 0.0 | 60S acidic ribosomal protein P1 |
| ROA1_MOUSE | 0.0 | 0.0 | 0.0 | 0.0 | 2.5 | 0.0 | Heterogeneous nuclear ribonucleo-protein A1 |
| RS13_MOUSE | 0.0 | 0.0 | 2.5 | 0.0 | 2.5 | 0.0 | 40S ribosomal protein S13 |
| RS16_MOUSE | 0.3 | 1.7 | 0.0 | 0.0 | 0.0 | 0.0 | 40S ribosomal protein S16 |
| RS2_MOUSE | 0.0 | 0.0 | 2.0 | 0.0 | 3.0 | 0.0 | 40S ribosomal protein S2 |
| RS3_MOUSE | 0.3 | 2.0 | 2.5 | 0.0 | 3.0 | 0.0 | 40S ribosomal protein S3 |
| RSSA_MOUSE | 0.0 | 2.0 | 0.0 | 0.0 | 3.0 | 0.0 | 40S ribosomal protein SA |
| SERPH_MOUSE | 0.0 | 0.0 | 0.0 | 0.0 | 0.0 | 6.0 | Serpin H1 |
| SETX_MOUSE | 0.0 | 5.3 | 3.0 | 0.0 | 3.0 | 0.0 | Probable helicase senataxin |
| SFPQ_MOUSE | 0.3 | 2.0 | 0.0 | 0.0 | 0.0 | 0.0 | Splicing factor, proline- and glutamine-rich |
| SVIL_MOUSE | 0.0 | 2.3 | 2.0 | 0.0 | 0.0 | 0.0 | Supervillin (Archvillin; p205/p250) |
| TERA_MOUSE | 0.0 | 0.0 | 0.0 | 0.0 | 0.0 | 3.0 | Transitional endoplasmic reticulum ATPase |
| THIM_MOUSE | 0.0 | 0.0 | 0.0 | 0.0 | 2.5 | 0.0 | 3-ketoacyl-CoA thiolase |
| TLN1_MOUSE | 0.0 | 2.0 | 0.0 | 1.0 | 0.0 | 7.0 | Talin-1 |
| TYSY_MOUSE | 0.0 | 2.0 | 0.0 | 0.0 | 2.5 | 0.0 | Thymidylate synthase |
| VIME_MOUSE | 1.0 | 10.3 | 0.0 | 0.0 | 11.5 | 0.0 | Vimentin |
| YBOX1_MOUSE | 0.0 | 2.0 | 0.0 | 0.0 | 0.0 | 0.0 | Nuclease-sensitive element-binding protein |
| PXN_MOUSE | 0.7 | 44.0 | 58.5 | 88 | 35.5 | 49 | Paxillin |

Data are presented as mean peptide spectral count.